

In-air Exchange of Small Payloads Between Multirotor Aerial Systems

Ajay Shankar, Sebastian Elbaum, and Carrick Detweiler

Department of Computer Science & Engineering
University of Nebraska-Lincoln, Nebraska, USA.

Abstract. Exchanging payloads between multiple vehicles is a challenging problem that finds applications in sustained monitoring and long-range payload transportation. In this paper, we take the problem one step further and explore the design and implementation of a system of aerial vehicles that can exchange a small cargo/payload while air-borne. The proposed approach exploits the hover-capabilities of multirotor vehicles, and works within the constraints and the challenges imposed by such a task (such as proximity and contact forces). It is also portable to a wide range of vehicles, and does not require custom flight maneuvers in order to be viable. A simulation framework is utilized to highlight the key challenges addressed by the system. We present detailed results from experiments conducted outdoors that demonstrate two vehicles exchanging a small 60 g payload unit between them.

1 Introduction

Multirotor unmanned aerial systems (UASs) have the geometry, stability, and maneuverability that makes them attractive platforms for transporting a variety of cargo payloads. They are, however, limited in their endurance. Hence it is natural that a number of applications can benefit by having multiple UASs collaboratively perform tasks. For instance, long-range payload transportation can be achieved by relaying the payload from one UAS to another. Likewise, UASs that collect data from onboard sensors by hovering for prolonged periods of time can benefit by having a second UAS take its place.

Multiple UASs engaging with the same payload has transformative applications, however, it has usually been studied indoors in varied contexts [1–3]. Outdoors, the most straightforward way to transfer a payload carried by one UAS to another is for the former to land and deposit the payload on a reliable terrain, and then for the latter to pick it up. This can be slow, oftentimes infeasible, and does not utilize the full capabilities of a multirotor vehicle/flight.

In this paper, we present the first steps towards transferring payload between two UASs *while* they are both air-borne. A system that allows aerial transfer of payloads can offer potential a speed-up over ground-based systems, while also enabling a transfer over regions where it may be impractical to land. Exchanging payloads mid-flight, however, is challenging due to the rich dynamics and the complexity of the process, as well as the impact of failures which are likely

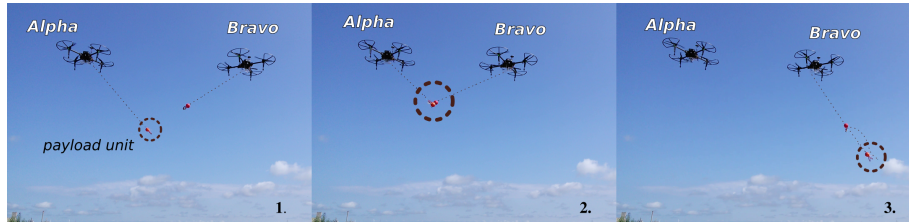


Fig. 1: Snapshots depicting the two vehicles *Alpha* and *Bravo* as they 1) approach each other, 2) intersect the payload strings, and 3) transfer the payload.

catastrophic for the UASs involved. Our proposed approach involves a controlled swinging of a payload system on both the sender and the receiver vehicles, as shown in Figure 1. The approach does not require custom flight controllers, which makes it broadly applicable to a wide variety of multirotors.

Numerous examples in the literature discuss multiple UASs collaboratively transporting a payload with a flexible number and geometry of the vehicles [3,4]. Previous work has also demonstrated the potential for two vehicles to exchange payloads by means of a deployed parachute [5]. Adding or removing mass from an aerial vehicle is typically limited to systems that allow swapping batteries [6], and manned aerial refueling [7]. While these involve multiple UASs tethered to the same object (or to each other), they do not specifically address the scenario of one vehicle handing off an object to another vehicle mid-air. Methods for swapping out batteries also typically follow the routine of land-exchange-takeoff. Another class of related work includes robotic arms and grippers that can manipulate objects [8,9]. Accessibility of the payload is one of the key challenges posed by the structural design of the moving parts of a multirotor. While robotic manipulators can work around this by extending outwards, they are usually limited in their reach. Additionally, positioning the payload becomes a greater challenge when it is extended far outwards from the body. The problem is aggravated outdoors as multiple vehicles must maintain precise relative positions. Furthermore, the controller must account for contact forces, which may be harder to estimate in the presence of environmental noise. It is evident that the task of exchanging payloads mid-air is inherently full of challenges, and few have explored this area.

Our proposed approach circumvents several of these concerns and reduces the risk imposed on the UASs. We show that it is possible to exchange payloads in-flight through physical experiments, and present simulations to explore some of the parameter space. We begin by quantifying the primary challenges involved and then defining our problem statement.

1.1 Challenges

Interaction between two simultaneously airborne vehicles outdoors has several challenges which can be grouped into three main classes:

1. *Separation between vehicles:* A mechanism that enables two vehicles to exchange payloads mid-air must maximize the distance of their closest approach. Given environmental uncertainties, hovering in close proximity will increase the risk of collision for the vehicles.

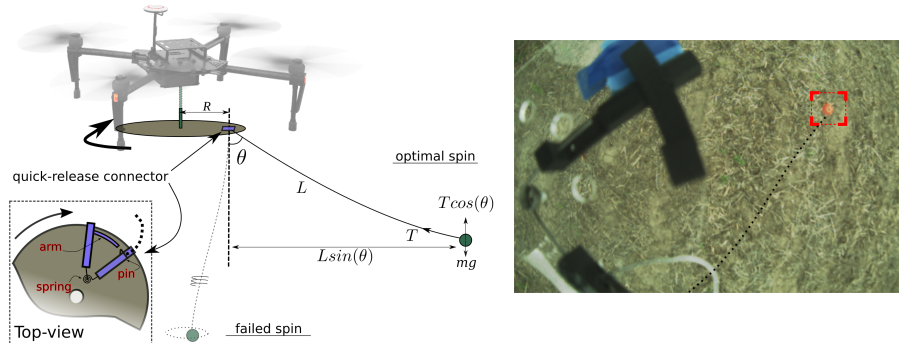


Fig. 2: *Left.* A diagrammatic representation of our approach for extending the payload far out from the UAS. The disc housing is rigidly affixed with a DC motor (not shown) to the body of the vehicle. As the disc spins, the vertical component of the tension in the string causes the payload to move on a conical pendulum with increasing θ . *Right.* The view from the downward facing camera with the payload and the cable highlighted for clarity.

2. *Accuracy in relative positioning:* To perform a payload hand-off, the vehicles will need to maintain extremely precise relative positions. In the absence of extremely accurate state estimates, this may be infeasible to achieve.
3. *Contact forces:* If the payload hand-off is not executed rapidly, the two vehicles in the process will be in contact with each other for a sustained period of time, which makes the joint dynamics very complex. Force-based flight controllers [10, 11] may be utilized to achieve some degree of compliance, however, state estimation still remains challenging outdoors.

1.2 Problem Statement

We are interested in developing a system that can enable the transfer of one unit of payload between two UASs, hereafter called *Alpha* and *Bravo*, while in hover. In addition, our goal is to impose minimal constraints on the choice and the design of the vehicles, and be able to function oblivious to the specific characteristics of the flight controller. Particularly, we require a setup that can operate without (and eliminates the need for): 1) having to land, 2) robotic end-effectors or manipulators that require precise positioning, 3) prolonged contact between two end-effectors, or 4) specialized flight controllers for 1, 2 or 3. To be practical, such a mechanism must provide reasonable guarantees of safety, while utilizing the capabilities of a multirotor.

2 Approach

Our approach enables two multirotors to exchange a unit of payload mid-air by extending it outwards from the body of the vehicle through a rotational motion. The extension enables the positioning of the vehicles with a safe separation between them, while the rotational element is designed such that the end-effectors need to be in contact very briefly, and a transfer can happen in spite of a lower precision in positioning.

Figure 2(left) shows a graphical representation of this system mounted underneath a UAS (*Alpha*). The payload is connected to a circular disc by means of a lightweight inelastic string. As a motor spins the disc, the payload is extended outwards as a function of θ , the half-angle of the inscribed conic. In an ideal steady-state, the relationship between the angular velocity of the payload (ω_p) and θ is governed by

$$g \tan(\theta) = (R + L \sin(\theta)) \cdot \omega_p^2,$$

where g denotes the acceleration due to gravity, R is the radius of the disc, and L is the length of the string used.

A critical challenge in practice is the possibility that the disc spins at a high speed while the payload simply dangles almost vertical (shown faded in Figure 2 left). Due to a flexible string and the two degrees of freedom at the joint between the string and the disc, the payload’s rotational velocity (ω_p) will not necessarily equal the disc’s rotational velocity (ω_d), and external disturbances (such as wind) can cause the payload to dangle vertical. To recover from such a state, the disc must slow down and ramp up its angular velocity such that the payload spins up “in phase.” We reason that feedback is then an essential element in the system design. First, it is critical for a spinning system subject to external disturbances such as the ones introduced by the UAS. Second, feedback helps in designing a system that is more accommodative of variations in R and L . In our implementation we employ visual feedback by means of a machine-vision camera and a compact onboard computer mounted on the UAS, described later.

Quick-release connector. One essential component of the design is a reliable mechanism for quickly disconnecting the payload from *Alpha*. There are two conflicting requirements on the design: 1) it must withstand the high tension in the cable during spinning, and 2) it must disengage upon a resistance that is both *external* (not caused by drag or inertia) and acts in the *same* direction as the tension. Our mechanism¹ for addressing these requirements, shown in Figure 2 (left), consists of a fixed bar and a movable pin that is loaded on a torsion spring. The arm of the pin has an adjustable length so that the sensitivity of the mechanism can be adjusted. During spinning, the tension on the cable compresses the spring to some extent. However, upon external contact, the higher cable tension compresses the spring further in order to dislodge the pin that holds the cable, thereby releasing the payload. The components are made of 3D printed nylon-onyx material, and are produced in our laboratory.

The string is connected to the disc through this quick-release connector which is designed to detach upon contact with any external impact that resists its spin. *Alpha* maintains a hover as the payload spins up, extending outwards at a distance of $R + L \sin(\theta)$ from the center of *Alpha*. A similar mechanism is mounted on the receptor vehicle (*Bravo*). This allows *Bravo* to position itself laterally adjacent to *Alpha*, and “snatch” the payload by having their strings intersect.

¹ Special thanks to Ashraful Islam for his contributions to the design.

Visual Feedback. We have emphasized the importance of feedback regarding the states of the disc and the payload in the reliability and the performance of the system. This can be accomplished by several means; however, in our implementations, we use visual feedback for its flexibility and ease of design. We do so by utilizing a downward facing camera mounted under the body of the vehicle (see Figure 2, right), and a vision processing algorithm that segments out the payload and the disc using color. The control input to the motor is a commanded rotational rate that increases with time. The algorithm measures the actual rotational rate of the disc (ω_d) and the payload (ω_p), and generates a commanded $\omega_d \pm \Delta\omega_d$ so as to minimize $(\omega_d - \omega_p) \bmod 2\pi$. In essence, the goal of this proportional controller is to ramp up the speeds of the disc and the payload while ensuring that they remain in phase. A pseudo-code for the algorithm is listed in Algorithm 1. The function s (line 3) represents the scale at which the commanded rate grows with time, and k is constant for proportionality.

Algorithm 1: Pseudo-code listing that controls the speed of the disc in order to ensure that the payload can be spun up reliably.

```

1 Procedure CTRL-DISC-SPEED:
  | Input :  $\omega_d, \omega_p, t$ 
  | Output: Commanded speed (cmd_rpm)
2  while mission_active do
3  |    $\omega \leftarrow s(t)$ 
4  |   if  $\neg$  IN-PHASE() then
5  | |    $\Delta\omega \leftarrow (\omega_d - \omega_p) \bmod 2\pi$ 
6  | |    $\omega \leftarrow \omega + k * \Delta\omega$ 
7  |   end
8  |   cmd_rpm  $\leftarrow \omega$ 
9  end

1 Function IN-PHASE():
2 | return  $|t_{d,ref} - t_{p,ref}| \leq t_{thresh,ref}$ 

```

To assess whether the disc and the payload are spinning in phase, the algorithm also measures $t_{d,ref}$ and $t_{p,ref}$, the times at which the disc and the payload cross an arbitrary reference line (*ref*) in the image plane. The helper function in Algorithm 1 uses a small constant ($t_{thresh,ref}$) to ensure that $t_{d,ref} \approx t_{p,ref}$. The variable *mission_active* is unset once the payload is disengaged from *Alpha*.

The proposed approach is generic and portable to a wide-range of multirotors. Generic slung-load control has been studied in the literature [12, 13], however, in order to conform to the problem statement we outlined, our system design functions completely oblivious to the choice of aircraft and flight controllers. Furthermore, our method also addresses the three primary challenges outlined in Section 1.1 – 1) the length of the two cables allows the vehicles to be separated well apart, 2) the vehicles can be in relative motion while transferring the payload, and 3) the quick-release connector minimizes the the interaction time between the two vehicles.

3 Simulation Study

To evaluate certain key behavioral characteristics of the system, we use a physics-based simulation framework designed in MATLAB Simulink[®]. Particularly, we investigate two matters: 1) the angular acceleration profile that must be commanded to the motor to ensure that the payload can be spun up, and 2) the value of using state feedback in this process. In the our simulations, we model the string as a series of short elements interlinked via elastic ball joints that mimic its experimentally observed physical characteristics. The motor and the disc are likewise modeled as physical objects connected via a revolute joint. We then simulate the rotation of the disc by gradually increasing the torque applied by the motor. Note that we do not attempt to model physical factors such as damping, friction, cable elasticity, etc.

Acceleration Profile. To spin the payload up, we command an angular acceleration, $\dot{\omega}_d(t)$, for the disc in the form of applied torque. Intuitively, $\dot{\omega}_d(t)$ must not be a step function if a sustained “in-phase” spin is desired. The failed spin shown as a faded illustration in Figure 2 (left) is one possible consequence of modeling $\dot{\omega}_d(t)$ as a step function. We hypothesize that a linear ramp (corresponding to $s(t) = c_1 t + c_2$, for some c_1 and c_2 , in Algorithm 1) would yield better results. However, the parameters of the ramp function are not known. Later on, we also consider the possibility that deviations from a steady ramp may be necessary.

In order to empirically find a suitable $\dot{\omega}_d(t)$, we utilize MATLAB’s Global Optimization Toolbox combined with our Simulink model to optimize its response. We first constrain the simulation to run only for a finite time period (T). This time period is further divided into n smaller intervals, and an applied torque is computed for each of these intervals. The optimization problem is given an initial guess in the form of a ramp function (c_1, c_2), and an n -element vector for applied torque is sought. The objective function minimizes

$$J(\theta(t), \phi(t)) = \int_0^T \phi(t) dt + \left(\frac{\pi}{2} - \theta(T)\right),$$

constrained to $0 \leq \theta(t) < \frac{\pi}{2}$. The variable $\phi(t)$ in the cost denotes the angular phase difference modulo 2π . Figure 3 shows the results from one sample optimization routine which was seeded with an initial guess of $c_1 = 0.026$ and $c_2 = 0.2$. The snapshots on the left graphically show the response of the system (comprised of a disc and a payload connected by a string) for the initial guess for $\dot{\omega}_d(t)$ and for the optimized $\dot{\omega}_d(t)$. The figures on the right also show the corresponding responses plotted. Note how small modifications to the linear ramp can produce dramatic differences in the response of the system.

In practice, it may be hard to solve for a desired $\dot{\omega}_d(t)$, even if all system parameters were known before hand. As mentioned before, environmental disturbances will further necessitate adjustments to $\dot{\omega}_d(t)$ in real-time, which further justifies the use of a feedback system. We also note that a mathematical model of this system is immensely complex, and therefore a reactive procedure listed in Algorithm 1 is well suited for our application.

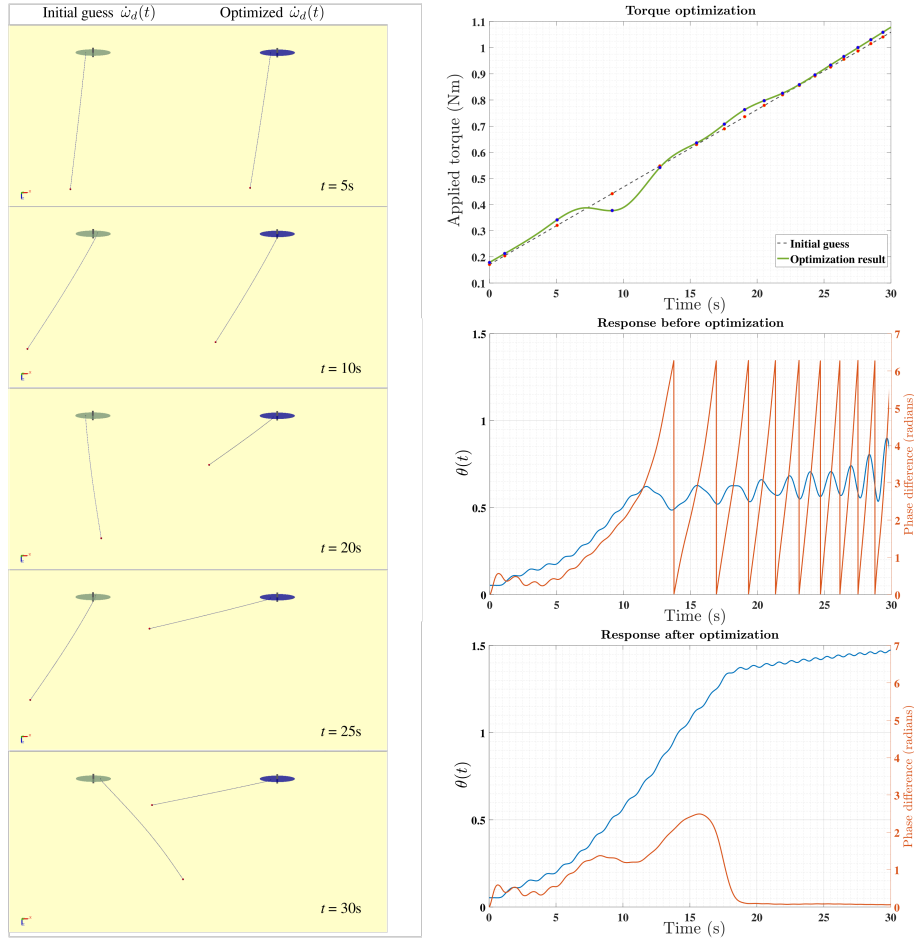


Fig. 3: Snapshots of the results from one optimization routine.

Feedback. In general, a particular acceleration profile, $\dot{\omega}_d(t)$, applied to systems with different combinations of the radius of the disc (R) and the length of the string (L) will not yield good results. In order to demonstrate the usefulness of feedback, we first define the $\dot{\omega}_d(t)$ that works well with our selected values of R and L . Then, the performance of the system is evaluated over a range of values of R and L . Since our intent is to maximize the separation between the vehicle and the payload, we inspect the maximum value of θ attained by the system.

The simulation is initialized at $\theta = 0$ (vertical cable) and $\omega_d = 0$. Figure 4 shows the maximum θ attained by the string when, for different values of R and L , a) the same $\dot{\omega}_d(t)$ is applied to the system (no feedback), and b) the selected $\dot{\omega}_d(t)$ is adjusted according to a feedback law. Clearly, without feedback, the string attains near-horizontal angles only for a very small range of values. However, the addition of a feedback control increases this range significantly, thereby improving the tolerance to disturbances. We also emphasize here that, in

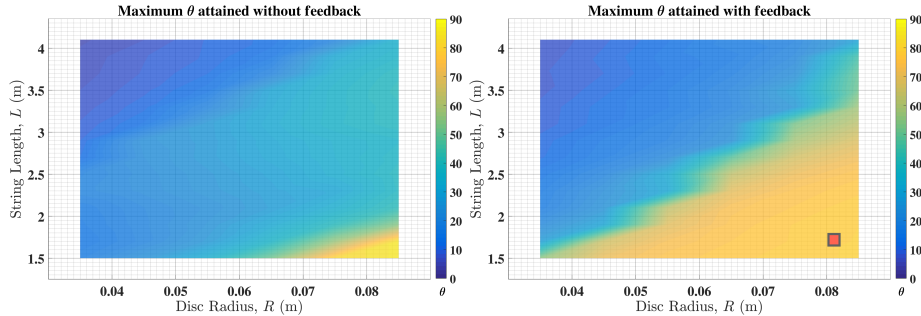


Fig. 4: Maximum θ attained by the string when the system is simulated over a range of values of R and L , (a) without, and (b) with feedback. The addition of feedback improves the tolerance of the system to variations in these parameters. The marked point (red) shows the values we use in our implementation.

practice, near-horizontal angles are generally unattainable outside of simulations because of physical imperfections of the systems involved.

4 Experiment Design

Through field experiments conducted outdoors, we are interested in assessing 1) how well the system can induce and sustain a spin in the presence of environmental disturbances and autopilot behavior, and 2) the feasibility of the actual transfer mechanism between two vehicles.

4.1 Hardware Implementation

We use a DJI Matrice 100 [14], a medium-scale quadcopter as our aerial platform. For our tests, we employ a solid payload that weighs approximately 60 g, connected to the disc using a lightweight nylon string of length (L) 1.6 m. The disc is cut out of acrylic and has a total radius (R) of 92 mm. It is spun by a 6 V brushless DC motor, which is rigidly affixed to the body of the vehicle. A downward-facing machine-vision camera (MatrixVision BlueFox, with a resolution of 752×480 px and approx. 110° horizontal field of view) mounted on the vehicle provides video feed to an Odroid XU4 (also on the vehicle). The Odroid observes the states of the disc and the payload and updates the rotational speeds commanded to the motor. We note here that entire setup is housed completely onboard the vehicle. Our approach is also independent of the choice of the multirotor and the flight controller, and does not require any specialized maneuvers by the vehicle, other than hovering.

Indoor and outdoor experiments are conducted to assess *Alpha*'s ability to induce and sustain the spin on a payload unit, and then transfer it to *Bravo*. Preliminary indoor tests are performed in unstructured environments that have no provisions for the UASs to maintain a position hold. The goal here is to ascertain that 1) the spinning mechanism can withstand disturbances induced by a non-stationary platform, and 2) the proposed system can function despite the vehicles not maintaining strict relative positions.

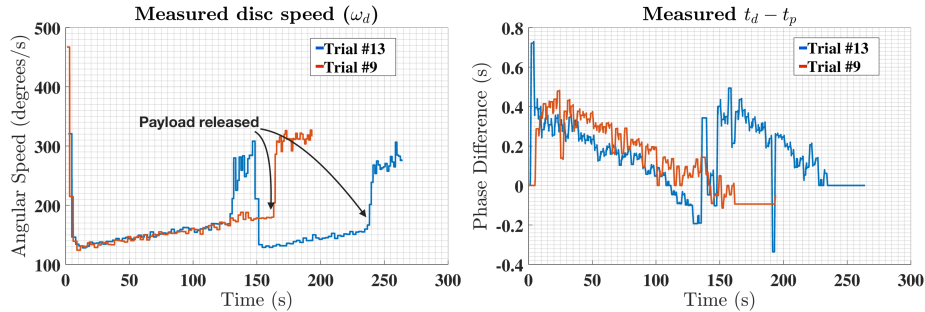


Fig. 5: The measured rotational speed of the disc, and the phase offset between the disc and the payload from two sample experiments (recorded on *Alpha*). When the payload is released, the disc has zero resisting torque which causes the spike in its speed. The phase difference starts at a positive value (the disc is “dragging” the payload) and then gradually approaches zero.

Both vehicles have identical builds, except for the quick-release connector (which is mounted only on *Alpha*), and *Bravo*’s payload (a dummy object which is similar to *Alpha*’s actual payload). In our experiments, both vehicles are piloted manually to approximately the same altitude above ground, while they begin spinning their respective attachments. As the payload approaches a steady spin, *Bravo* proceeds to approach *Alpha* horizontally in order to let their strings intersect. As the payload disengages from the quick-release connector on *Alpha*, it is trapped in the string affixed to *Bravo*. Figure 1 shows frames from an actual experiment in which *Bravo* (right) a) approaches *Alpha* that is already spinning the payload, b) interrupts the spin, thereby intercepting the payload and finally c) moves away with the payload.

5 Results

We begin by investigating how well the systems can spin up the payload outdoors. As listed in Table 1, the time taken to spin up the payload is fairly consistent for most of our trials. Figure 5(left) shows the gradually increasing measured rotation speeds of the disc from two sample tests. The figure on the right shows the phase offset between the disc and the payload (measured in seconds). In the beginning, this offset is positive, and as the payload gets in phase with the disc, this offset approaches zero. Starting from completely vertical, the time taken to get the payload up to its maximal extent is similar for the tests (unless influenced by strong external factors). However, as seen in Figure 5, the time that *Alpha* continues to spin the payload can be different for the tests. This can be either because *Bravo* does not intercept the payload right away, or because the contact force does not disengage the payload in the first attempt. In such a scenario (trial #13), *Alpha* simply restarts its spin. The sharp increase in the rotational speed of the disc is caused by the lack of resisting torque (load) on the disc after the payload is released (or restarts from vertical).

In a complete autonomous mission, the vehicles will need to hover adjacent to each other for some finite amount of time before the transfer is successful. Two properties of the system that are of interest are, then, the time it takes for *Alpha* to spin the payload up to its maximum extent (starting from completely vertical), and the approximate distance between the payload and *Alpha*'s center. Table 1 lists these two variables, along with *Alpha*'s waiting time for 16 sample tests we performed outdoors. All but one of the tests resulted in a successful disengagement of the payload from *Alpha*; and out of these, *Bravo* was able to successfully retain the payload in ten missions. The table also lists the number of attempts the system needed to make before the payload was disengaged. Majority of the missions took one attempt; however, trial #16, which suffered strong gusts of wind required 4 attempts before both vehicles reached a steady state of spin. For the rest of the missions that took more than one attempt, both *Alpha* and *Bravo* simply reset their spinning mechanisms. Note that in manual missions, the waiting time is dependent on the readiness of *Bravo*. Also, as we note in trial #6, there's a possibility that the payload does not release at all if it collides with *Bravo*'s dummy object (instead of the strings intersecting).

Table 1: The total mission time, split into spin time and the waiting time (for *Alpha*), along with the approximate payload separation and number of transfer attempts made in 16 flights.

Trial	Spin Time (s)	Wait Time (s)	Total (s)	Dist (m)	# attempts	Notes
1	117	20	137	1.3	1	–
2	131	118	249	1.2	2	Drop
3	117	119	236	1.0	1	
4	120	44	164	1.3	1	Drop
5	150	120	270	1.3	2	
6	143	137	279	1.2	2	No release
7	120	34	154	1.2	1	
8	117	21	138	1.2	1	Drop
9	120	44	164	1.4	1	Drop
10	115	26	141	1.2	1	
11	120	34	154	1.4	1	Drop
12	118	67	186	1.4	1	
13	146	96	241	1.0	2	
14	117	36	153	1.3	1	
15	117	18	135	1.2	1	
16	485	110	594	1.0	4	
Mean	147.0	65.29	212.29	1.24	–	
Median	120.0	44.15	164.15	1.23	–	

6 Discussion

One of the key insights from our simulations is the relevance of feedback in the mechanism that spins the payload. For a system that must work with a range of parameters (R , L , and the weight of the payload), and in different environmental conditions, it is necessary to have a controller that can adapt the rate of spin even if many of those parameters are known beforehand.

Even though our method only requires the vehicles to hover, it is imperative that the torques exerted due to the spinning motion remain within critical limits. While spinning, the payload’s momentum may induce rotations on the body of the vehicle. Figure 6 shows the 3-axis gyroscope readings from the vehicle’s onboard IMU during one representative test mission. The spinning mechanism is initiated at approximately 160 s and is active throughout the highlighted region. We notice that as time progresses (i.e., the rotation speed increases), the effect becomes increasingly pronounced. At the peak (approx. 430 s), the measured rotation rate is close to $8^\circ/\text{s}$. Even though it is noticeable, the effect is small (approx. 2.5%) compared to the maximum angular velocity that our particular vehicle and flight controller can attain. We also note that since this is, in general, a function of the mass and the rotational speed of the payload, an appropriate choice of vehicle can be made by considering its hover performance.

Surprisingly, the motion of *Alpha* did not have a significant impact on the way the payload is spun up. We expected that deviations from a perfect hover would deteriorate the spin; however, from our preliminary tests, which were performed indoors (GPS-denied, no position hold) we found that the performance of the system does not change significantly. It was empirically determined that due to environmental disturbances such as wind, only the rate at which the rotational speed of the disc is increased needed to be altered (the factor s in Algorithm 1). This value was decreased, so as to allow the system to spin up less aggressively. Our experiments were conducted in winds of up to 3 m/s (the range within which the vehicles do not exhibit significant drifts in altitude). Since the string will not be perfectly horizontal, the shape of the conic inscribed by it allows a difference in altitude of approximately 1 m. Nevertheless, we acknowledge that one limitation of our method is that a significant drift in altitude by one vehicle may pose a threat to the other.

Surprisingly, the motion of *Alpha* did not have a significant impact on the way the payload is spun up. We expected that deviations from a perfect hover would deteriorate the spin; however, from our preliminary tests, which were performed indoors (GPS-denied, no position hold) we found that the performance of the system does not change significantly. It was empirically determined that due to environmental disturbances such as wind, only the rate at which the rotational speed of the disc is increased needed to be altered (the factor s in Algorithm 1). This value was decreased, so as to allow the system to spin up less aggressively. Our experiments were conducted in winds of up to 3 m/s (the range within which the vehicles do not exhibit significant drifts in altitude). Since the string will not be perfectly horizontal, the shape of the conic inscribed by it allows a difference in altitude of approximately 1 m. Nevertheless, we acknowledge that one limitation of our method is that a significant drift in altitude by one vehicle may pose a threat to the other.

7 Conclusion

This paper presents an approach for two multirotor UASs to exchange their cargo payloads in air. We demonstrate the system’s capabilities through outdoor field experiments, and present a detailed analysis of the results. We noted earlier that our proposed approach is contained entirely onboard the UAS, and has no dependencies on external resources such as a motion capture system or custom flight controllers. In the future, we wish to make the process entirely autonomous,

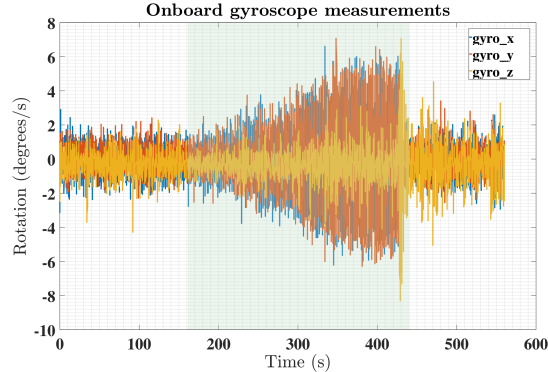


Fig. 6: The progression of 3-axis gyroscope measurements as the payload is spun up (shaded area between 160 s to 430 s).

and towards that end, we have already conducted some field trials with missions that have shared autonomy.

References

1. Su, K., Shen, S.: Catching a flying ball with a vision-based quadrotor. In: International Symposium on Experimental Robotics. pp. 550–562. Springer (2016)
2. Ritz, R., Müller, M.W., Hehn, M., D’Andrea, R.: Cooperative quadcopter ball throwing and catching. In: Intelligent Robots and Systems (IROS), 2012 IEEE/RSJ International Conference on. pp. 4972–4978. IEEE (2012)
3. Sreenath, K., Kumar, V.: Dynamics, control and planning for cooperative manipulation of payloads suspended by cables from multiple quadrotor robots. *Robotics: Science and Systems* (2013)
4. Jiang, Q., Kumar, V.: The inverse kinematics of cooperative transport with multiple aerial robots. *IEEE Transactions on Robotics* 29(1), 136–145 (2013)
5. Shankar, A., Elbaum, S., Detweiler, C.: Towards Aerial Recovery of Parachute-Deployed Payloads. In: Intelligent Robots and Systems (IROS), 2018 IEEE/RSJ International Conference on. IEEE (2018)
6. Wang, M.: Systems and methods for UAV battery exchange (May 24 2016), US Patent 9,346,560
7. Smith, R.K.: Seventy-five years of inflight refueling. Ohne Verlagsangabe. Washington (1998)
8. Kim, S., Choi, S., Kim, H.J.: Aerial manipulation using a quadrotor with a two dof robotic arm. In: Intelligent Robots and Systems (IROS), 2013 IEEE/RSJ International Conference on. pp. 4990–4995. IEEE (2013)
9. Jimenez-Cano, A., Martin, J., Heredia, G., Ollero, A., Cano, R.: Control of an aerial robot with multi-link arm for assembly tasks. In: Robotics and Automation (ICRA), 2013 IEEE International Conference on. pp. 4916–4921. IEEE (2013)
10. Parra-Vega, V., Sanchez, A., Izaguirre, C., Garcia, O., Ruiz-Sanchez, F.: Toward aerial grasping and manipulation with multiple UAVs. *Journal of Intelligent & Robotic Systems* 70(1-4), 575–593 (2013)
11. Augugliaro, F., D’Andrea, R.: Admittance control for physical human-quadcopter interaction. In: Control Conference (ECC), 2013 European. pp. 1805–1810. IEEE (2013)
12. Palunko, I., Fierro, R., Cruz, P.: Trajectory generation for swing-free maneuvers of a quadrotor with suspended payload: A dynamic programming approach. In: Robotics and Automation (ICRA), 2012 IEEE International Conference on. pp. 2691–2697. IEEE (2012)
13. Guerrero, M., Mercado, D., Lozano, R., García, C.: Passivity based control for a quadrotor UAV transporting a cable-suspended payload with minimum swing. In: Decision and Control (CDC), 2015 IEEE 54th Annual Conference on. pp. 6718–6723. IEEE (2015)
14. DJI Matrice 100. <http://www.dji.com/matrice100>, [Online; accessed August 2018]